CHARACTERIZATION OF THE EMISSION FROM 2D ARRAY JOSEPHSON OSCILLATORS *

P. A. A. Booi and S. P. Benz

Abstract-- We present experimental results on the emission from phase-locked two-dimensional arrays of Josephson junctions. We have coupled the emission from 10 x 10 arrays to a room-temperature mixer through a fin-line antenna and WR-12 waveguide. A single voltage-tunable peak was detected up to 230 GHz. A stripline resonance in the antenna reduced the array's dynamic resistance and thereby the emission linewidth to as low as 10 kHz. We extract an effective noise temperature of 14 K from the linewidth data. When the array's emission was coupled to an on-chip detector junction through a dc blocking capacitor, we detected voltage-tunable emission from 75 GHz up to 300 GHz, and in some circuits emission above 400 GHz. The coherent power spectrum depends primarily on internal resonances.

I. INTRODUCTION

Josephson junctions are natural voltage-tunable oscillators with characteristic frequencies in the GHz and THz frequency range. For applications such as on-chip local oscillators (LOs) for mixers, powers of ~1 μW and linewidths less than 1 MHz are required. Three types of Josephson oscillators, flux flow oscillators (FFOs),[1,2] one-dimensional (1D) arrays,[3-5] and two-dimensional (2D) arrays of Josephson junctions,[6-9] have generated enough power to pump an on-chip mixer. For off-chip applications, higher power, >1 mW coupled to a 50 Ω load, is required. 1D and 2D arrays are theoretically capable of delivering such power at GHz and THz frequencies.

Since the demonstration of coherent voltage-tunable emission from phase-locked 2D arrays,[6] considerable research has been devoted to understanding the phase-locking mechanism. Wiesenfeld *et al.*[10] analytically showed that unloaded 2D arrays exhibit stable phase locking between parallel junctions in a given row, but only neutrally stable phase locking between rows. This result is reminiscent of unloaded 1D series arrays where the phase-locked state is neutrally stable.[11] In 1D arrays, a weak interaction, such as feedback through a load, can induce phase locking. Similarly, phase locking between the N rows (each having M junctions in parallel in the voltage state) in 2D arrays can be stabilized by a load. Darula *et al.*[12] and Kautz[13] have observed

---

This work was partially supported by the BMDO Office of Innovative Science and Technology with technical program management from Rome Laboratory, and partially supported by the Office of Naval Research. P. A. A. Booi acknowledges the support of the University of Twente in The Netherlands.

The authors are with the National Institute of Standards and Technology, Boulder, CO 80303.

stable in-phase states in simulations of 2D arrays coupled to resistive loads. 2D arrays can compensate for $\sqrt{M}$ times more critical current disorder than 1D arrays.[13] This results from the inherent ability of current redistribution in 2D arrays to compensate for non-uniformities in the junction parameters.

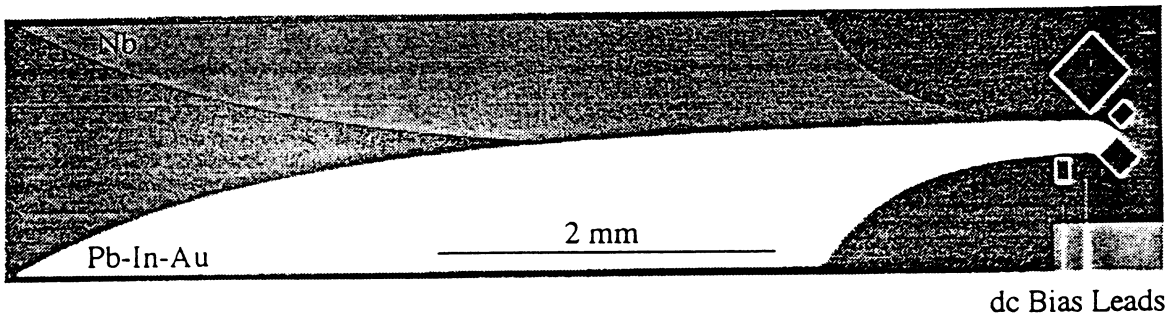

Fig. 1: Photograph of a 10 x 10 array (right) coupled to a fin-line antenna (left). The photograph also shows other arrays that are connected to antennas on other chips on the 7.62 cm (3 in) wafer.

We have characterized the emission from 2D array oscillators coupled to two different detection circuits. In the off-chip detector circuit (see Fig. 1), the arrays are coupled to a room-temperature mixer through a fin-line antenna and WR-12 (60-90 GHz) waveguide.[14] For on-chip detection, the arrays are coupled to a detector junction through a dc blocking stripline capacitor.[15] All arrays discussed in this paper use ground planes to reduce self-field effects and 4 x 4 μm^2 junctions (unless mentioned otherwise) . Linewidth, power, and tunability of the emission are discussed in terms of circuit resonances. These data provide useful design criteria for higher-power array designs.

II. TWO-DIMENSIONAL ARRAYS OF JOSEPHSON JUNCTIONS

When current-biased at average voltage V, the supercurrent of a single resistively shunted junction (RSJ) oscillates at frequency $\nu_1^j = V/\Phi_0$, where $\Phi_0 = h/2e$, h is Planck's constant, and -e is the elementary electron charge. For low normalized bias voltages $v = V/I_cR < 1$ (I_c is the critical current and R is the resistance of the RSJ), the junction generates harmonics with frequencies $\nu_n^j = nV/\Phi_0$, where n = 1, 2, 3, ... The junction can deliver a power

$$P_n^j = \frac{(v_n I_c R)^2 R_L}{2(R+R_L)^2} \qquad (1)$$

to a resistive load R_L for each nth harmonic at a given bias voltage.[3] The normalized harmonic amplitudes v_n are given by

$$v_n = \frac{2v}{(i+v)^n}, \tag{2}$$

where $i = I/I_c$, I is the bias current, and v is defined as $v = V(R+R_L)/I_cRR_L$ when the load directly shunts the junction. For $v > 1$, thus v greater than the characteristic frequency $\nu_c = I_cR/\Phi_0$, the junction oscillations are almost sinusoidal (higher harmonics are negligible) and the junction can deliver a fundamental power $P_1^j = I_c^2R/8$ to a matched load $R_L = R$. The theoretical linewidth of the oscillations, given by the full width at half-maximum power, is[16,17]

$$\Delta\nu_n^j = \pi\,(nR_d/\Phi_0)^2\,\{S_I(0) + [S_I(V)/2i^2]\} \tag{3}$$

where $S_I(V) = (4eV/R)\coth(eV/kT)$, $R_d = dV/dI$ is the dynamic resistance of the RSJ, k is Boltzmann's constant, and T is the temperature. Equation (3) describes the linewidth in terms of the low-frequency noise spectrum, where Johnson noise $S_I(0) = 4kT/R$ and noise mixed down from the harmonic frequencies ν_n^j are included.

The inset of Fig. 2 shows a schematic of a 4 x 3 (M x N) array where 12 junctions can be in the voltage state and thus contribute to the emission. When M x N junctions in an array of RSJs phase lock, the power at array oscillation frequency ν_n^A delivered to a matched load $R_L = NR/M$ increases in proportion to (M x N) and the linewidth decreases in proportion to 1/MN.[3,7] Thus, for $v > 1$,

$$P_1^A = MNI_c^2R/8 = M^2I_c^2R_L/8, \tag{4a}$$

and

$$\Delta\nu_1^A = \frac{\Delta\nu_1^j}{MN}. \tag{4b}$$

Eq. (4b) holds provided that the individual junctions are identical (the array dynamic resistance $R_d^A = R_d$) and the array dimensions are much smaller than the fundamental wavelength, so that the array can be considered a lumped element.

Next we present experimental results that demonstrate the influence of junction parasitics and complex loads on the behavior of 2D array oscillators. When junction parasitics, such as the junction capacitance C_j and the inductance of each junction's shunt resistor L_s, are included, the equations that describe the junction dynamics cannot be solved analytically. Wiesenfeld *et al.*[10] have derived an analytic approximation for ν_1 which we use to estimate the power coupled to the detectors.

III. RESULTS

A. Off-chip detection of 2D array emission

Figure 1 shows a photograph of a 10 x 10 array. The array design has been discussed elsewhere.[7-11] The array is coupled to a 6.3 mm long antipodal fin-line antenna. The antenna is used to couple the array emission to the TE_{10} mode in WR-12 waveguide. The antenna transforms the array impedance into the waveguide impedance through two exponentially tapered fins.

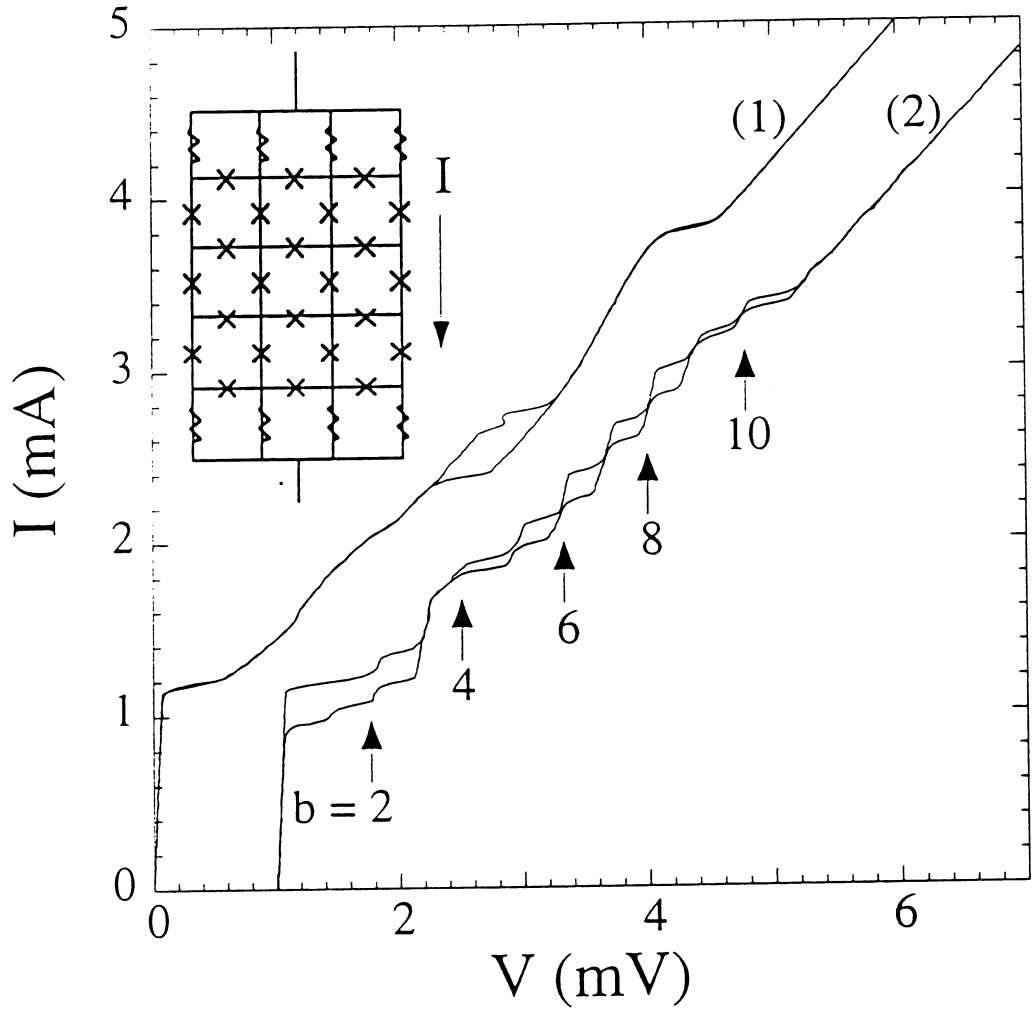

Fig. 2: I-V curve of a 10 x 10 array without (1), and with (2) the antenna. Curve (2) is displaced by 1 mV. Some of the resonance bands b are indicated with arrows. The inset shows a schematic of a 4 x 3 array where the junctions are shown as crosses.

Figure 2 compares the current-voltage (I-V) curves for an array with and without the antenna. The antenna induces in the I-V curve resonant steps that are independent of chip placement in the waveguide. The structure results from resonances in the ~3.3 mm overlapping region of the two fins at frequencies $\nu_R = b\, c_0/(6.6\text{ mm}) = b \times 17.4$ GHz. Here, $c_0 = 1.15 \times 10^8$ m/s is the phase

velocity and b is the number of half-wavelengths in the overlapping region. The resonances induce small tunable frequency bands (bands b identified in Fig. 2) with reduced dynamic resistance R_d^A in the I-V curve. Coherent emission is observed from these bands.

We detected a single voltage-tunable peak at frequencies up to 230 GHz for each bias voltage. The detection methods are discussed in Ref. 14. The frequencies of the emission peaks agree through the Josephson relation with the bias voltages. In Fig. 3, an example spectral peak from band 5 with a linewidth of ~13 kHz is shown. In general, the linewidth varies by an order of magnitude over the bands. For low b, we found that the measured linewidth scales with $(R_d^A)^2/R$ at each bias point. The proportionality factor between $\Delta\nu_1^A$ and $(R_d^A)^2/R$ (see Eqs. (3) and (4)) corresponds to an effective noise temperature of 14 ± 2 K.[14]

We detected a power of -88 ± 2 dBm across band 5 with a WR-10 harmonic mixer. We estimate the stripline-to-mixer loss of 8 ± 1 dB (including the stripline-to-waveguide loss of 4 ± 1 dB) from Shapiro steps induced in the I-V curve at 75 GHz with a Gunn LO. When corrected for this loss, and a mixer conversion and insertion loss of 43 dB, we arrive at an emitted power of -37 ± 3 dBm. The emitted power agrees with the theoretical power of -36.9 dBm (about 0.2 μW) from Eq. (4a). In general, we found the emitted and theoretical powers to be within a factor of 2.

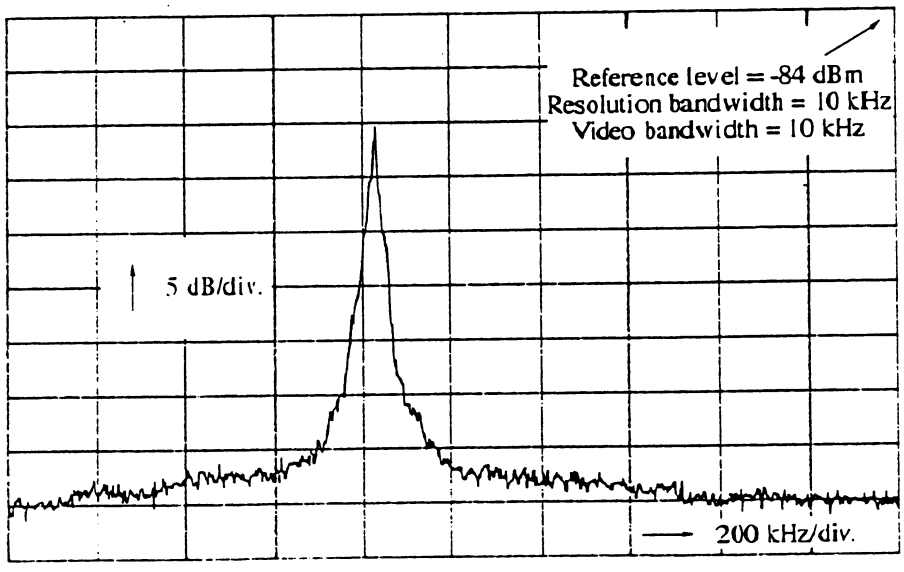

Fig. 3: Emission peak from band 5 after 100 video averages at 88.844 GHz showing a ~ 13 kHz linewidth.

The measured power and linewidth are consistent with the theoretical model in which all junctions phase lock. We detected linewidths as low as 10 kHz, which are the lowest linewidths reported for Josephson oscillators. Coherent emission was observed up to 230 GHz. This frequency range is limited by the low-pass character of the junction capacitance C_j ~0.64 pF. We expect stripline losses to limit the frequency range of arrays with smaller junctions (smaller C_j).

B. On-chip detection of 2D array emission

Next, we discuss circuits where external resonances are eliminated. For example, the stripline capacitors (that are used to couple the array's emission to a detector junction) were designed so that no standing waves occurred at the frequencies of interest.[8] In this way, the measured spectra reflect array characteristics but no external resonances. The data show no significant features introduced by the load that are not related to internal resonances. This does not mean that the phase-locked state is not influenced by feedback through an external load, but that the main features of the emission spectrum are determined by internal resonances.

Figure 2 shows the I-V curve of an unloaded 2D array [curve (1)]. The structure in this I-V curve results from resonances between C_j and a combination of L_s and the array cell inductance L. Similar structure is observed in the I-V curves of loaded arrays. Figure 5, for example, shows the measured I-V curve of a 20 x 20 array coupled to a detector junction through a 75 x 300 μm^2 stripline capacitor.

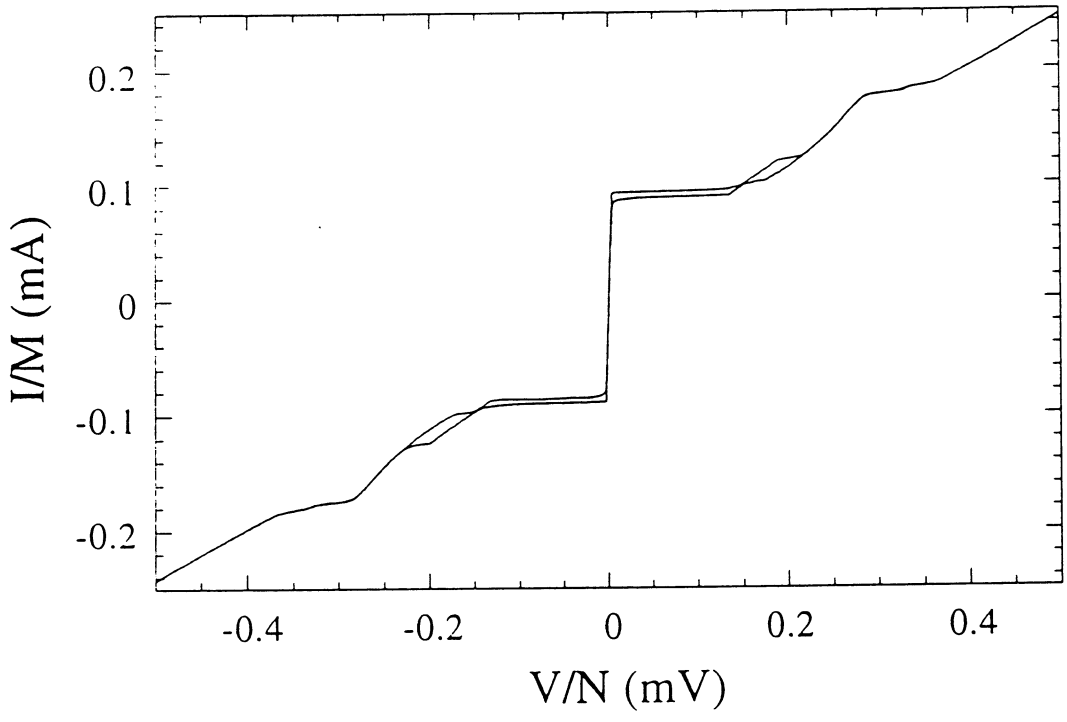

Fig. 5: Measured I-V curve of a 20 x 20 array coupled to a detector junction.

Figure 6 shows $R_d^A = dV/dI$ and the direct-detected power from the 20 x 20 array versus normalized array voltage V/N. The direct-detected power is determined by biasing the detector junction below (or above) the gap voltage (2.75 mV for Nb/AlO_x-junctions), so that emission is detected when the detector voltage V_d decreases (or increases).[19] Emission observed from such arrays at frequencies above 400 GHz is not shown in Fig. 6.

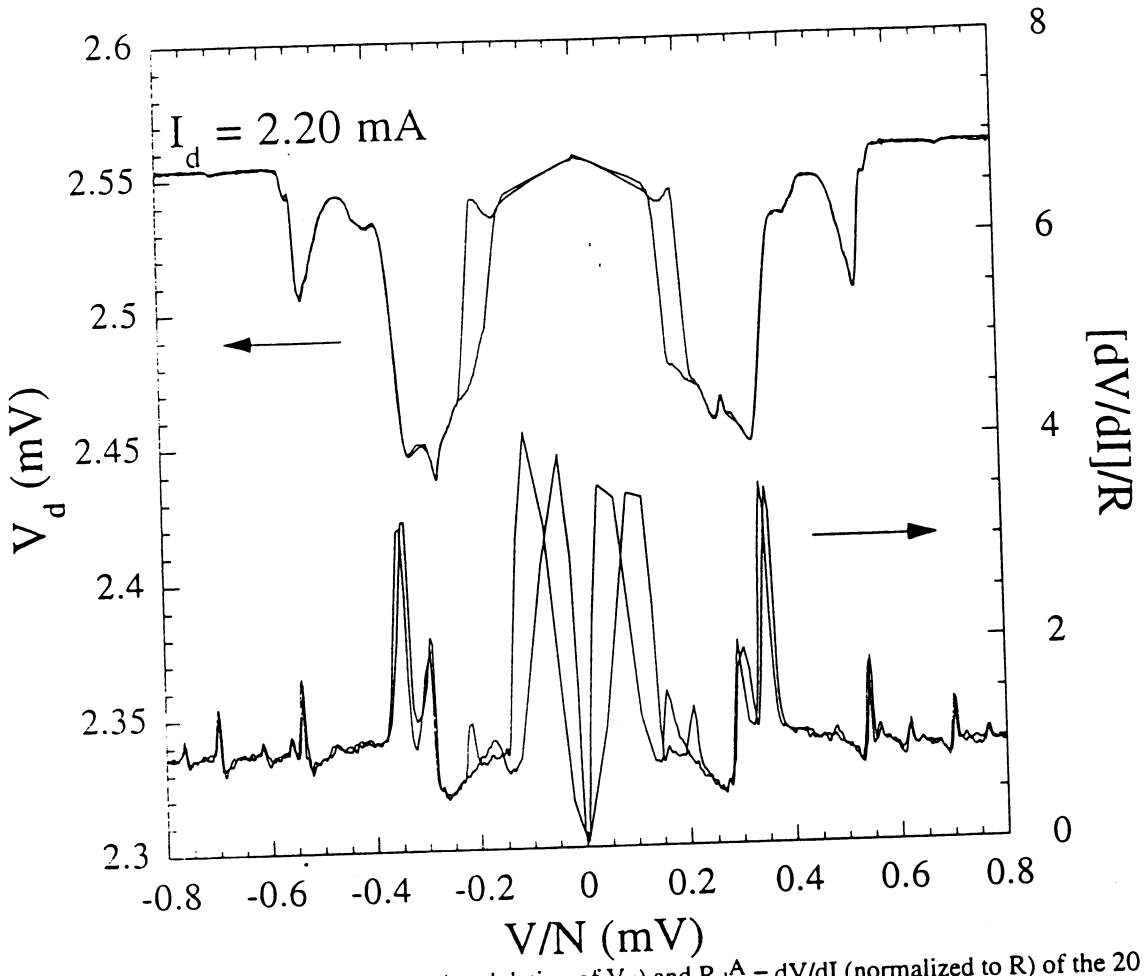

Fig. 6: Measured direct-detected power (modulation of V_d) and R_d^A = dV/dI (normalized to R) of the 20 x 20 array.

The low-voltage structure (V/N < 0.2 mV) in Fig. 5 which displays metastable states is thought to be related to vortex and anti-vortex propagation going back and forth across the array.[18] No coherent emission is detected at these voltages. This vortex motion may be similar to zero-field steps in 1D parallel arrays (which depend on L and C_j) and will be discussed in Ref. 15. Coherent emission is observed for V/N ≥ 0.2 mV ($\nu \geq \nu_c$).

The structure in Fig. 5 for V/N ≥ 0.2 mV is predominantly determined by a (junction) resonance between the shunt resistor's inductance L_s and the junction's capacitance C_j; this resonance determines the primary (coherent) emission band. Fig. 6 shows that this primary emission band occurs for V/N (approximate frequency) varying from 0.2 (90 GHz) to 0.35 mV (170 GHz). This range is the same for 6 x 6 and 10 x 10 arrays, both with and without horizontal junctions perpendicular to the bias direction. This feature also occurs for arrays with different cell inductance, and in circuits with different coupling structures.

Our data indicate that the low frequency limit of the primary emission band is ν_c, and the high-frequency limit is approximately the parasitic junction resonance near $\nu_r = 1/2\pi\sqrt{L_sC_j} = 152$ GHz (L_s = 1.7 pH and C_j = 0.64 pF). Beyond this resonance, the I-V curve shows a high-R_d^A transition back to V = RI (near V/N = 0.35 mV in Fig. 6). For arrays with larger L_s = 2.4 pH (larger dielectric thicknesses), ν_r decreased to ~128 GHz. For arrays with smaller junctions (smaller C_j), the primary emission band occurred up to higher ν_r; for example, arrays with 2 x 2 μm^2 junctions have a primary emission band up to 300 GHz. For arrays with larger ν_c, the onset of coherent emission is shifted to higher frequencies, which explains the lack of coherent emission observed from arrays with high junction I_c when $\nu_c > \nu_r$.[7]

From the quality factor of the junction resonance $Q = \nu_r/\Delta\nu = \sqrt{L_s/R^2C_j}$, we obtain a corresponding bandwidth $\Delta\nu = R/2\pi L_s$ = 133 GHz. Above the primary emission band, emission is observed predominantly at multiples of ν_r with detected powers decreasing as $(\nu/\nu_r)^{-2}$. This decreased power for higher frequencies follows the transfer characteristic of the parasitics.

Our data from on-chip detection circuits show no significant features introduced by the load that are not related to resonances intrinsic to the array circuit. Frequency bands of coherent emission seem to be determined primarily by the resonance between junction parasitics L_s and C_j. The detected power at all frequencies corresponds to all junctions being phase locked. The oscillator is tunable over a primary emission band that ranges in frequency from approximately ν_c to slightly beyond ν_r. Thus, the desired emission characteristics of 2D arrays based on shunted tunnel junctions can be determined through modeling of the resonances between these parasitics.

IV. DISCUSSION AND CONCLUSIONS

The emission spectra of 2D arrays are strongly dependent on resonances external and internal to the array. We observe coherent emission near multiples of the resonance frequencies. When the structure coupled to antennas, the emission is dominated by the external resonances in the antenna. When the arrays are not coupled to the antenna, for example, when the arrays are coupled to on-chip detector junctions, internal resonances in the array due to junction parasitics determine the emission spectra. Characterization of external and internal resonances is necessary for accurate prediction of power, linewidth, operating frequency, and tunability of phase-locked Josephson arrays.

The L_sC_j resonance can be useful in maximizing the power delivered to a load, but at high frequencies this will limit tunability. Minimization of circuit parasitics is necessary for higher-power, higher-frequency Josephson oscillators so that both the tunability and operation of 2D array Josephson oscillators are increased. Thus, understanding junction parasitics is important in designing stable phase-locked 2D arrays.

ACKNOWLEDGMENTS

We thank E. N. Grossman, C. A. Hamilton, R. L. Kautz, R. H. Ono, C. D. Reintsema, A. V. Ustinov, M. P. Weidman, and K. A. Wiesenfeld for advice, discussions, and the use of equipment.

REFERENCES

1 A. V. Ustinov, T. Doderer, R. P. Huebener, J. Mygind, V. A. Oboznov, and N. F. Pedersen, "Multi-fluxon effects in long Josephson junctions," *IEEE Trans. Appl. Supercon.*, vol. 3 (1), pp. 2287-2290, March 1993.

2 Y. M. Zhang, D. Winkler, and T. Claeson, "Linewidth measurements of Josephson flux-flow oscillators in the band 280-330 GHz," *Appl. Phys. Lett.*, vol. 62 (24), pp. 3195-3197, June 1993.

3 A. K. Jain, K. K. Likharev, J. E. Lukens, and J. E. Sauvageau, "Mutual phase-locking in Josephson junction arrays," *Phys. Rep.*, vol. 109 (6), pp. 309-426, 1984.

4 B. Bi, S. Han, and J. E. Lukens, "Radiation linewidth of phase-locked distributed array in the submillimeter wave range," *Appl. Phys. Lett.*, vol. 62 (22), pp. 2745-2747, May 1993.

5 S. Han, B. Bi, W. Zhang, and J. E. Lukens, "Demonstration of Josephson effect submillimeter wave sources with increased power," *Appl. Phys. Lett.*, vol. 64 (11), pp. 1424-1426, March 1994.

6 S. P. Benz and C. J. Burroughs, "Coherent emission from two-dimensional Josephson junction arrays," *Appl. Phys. Lett.*, vol. 58 (19), pp. 2162-2164, April 1991.

7 S. P. Benz and C. J. Burroughs, "Two-dimensional arrays of Josephson junctions as voltage tunable oscillators," *Proceedings of the Third International Superconductive Electronic Conference*, Glasgow, pp. 230-237, June 1991; *Supercon Sci. Technol.*, vol. 4, pp. 561-56 1991.

8 P. A. A. Booi, S. P. Benz, T. Doderer, D. Hoffmann, J. Schmidt, S. Lachenmann, and R. Huebener, "Frequency dependence of the emission from 2D array Josephson oscillators," *IE Trans. Appl. Supercon.*, vol. 3 (1), pp. 2493-2495, March 1993.

9 M. J. Wengler, B. Guan, B. Liu, and E. K. Track, "190 GHz radiation from a quasiopt Josephson junction array," *Appl. Phys. Lett.*, submitted, 1994.

10 K. Wiesenfeld, S. P. Benz, and P. A. A. Booi, "Phase-locked oscillator optimization for ar of Josephson junctions," *J. Appl. Phys.*, submitted, 1994.

11 P. Hadley, "Dynamics of Josephson junction arrays," *PhD thesis*, Stanford Unive unpublished, 1989.

[12] M. Darula, P. Seidel, J. von Zameck Glyscinski, A. Darulova, F. Busse, and S. Benacka, "The stability of the phase-locked state in structures containing arrays of Josephson junctions," *EUCAS'93*, Göttingen, submitted, 1993.

[13] R. L. Kautz, "Phase locking in two-dimensional Josephson-junction arrays: Effect of critical-current nonuniformity," to be presented at *ASC'94*, Boston, MA, October 1994.

[14] P. A. A. Booi and S. P. Benz, "Emission linewidth measurements of two-dimensional array Josephson oscillators," *Appl. Phys. Lett.*, vol. 64 (16), pp. 2163-2165, April 1994.

[15] P. A. A. Booi and S. P. Benz, "Resonances in two-dimensional Josephson-junction arrays," *J. Appl. Phys.*, submitted, 1994.

[16] K. K. Likharev and V. K. Semenov, "Fluctuation spectrum in superconducting point junctions," *JETP Lett.*, vol. 15, pp. 442-445, 1972.

[17] R. H. Koch, D. J. Van Harlingen, and J. Clarke, "Quantum-noise theory for the resistively shunted Josephson junction," *Phys. Rev. Lett.*, vol. 45 (26), pp. 2132-2135, December 1980; "Observation of zero-point fluctuations in a resistively shunted Josephson tunnel junction," *ibid.* vol. 47 (17), pp. 1216-1219, October 1981.

[18] S. G. Lachenmann, T. Doderer, R. P. Huebener, P. A. A. Booi, and S. P. Benz, Observation of vortex motion in two-dimensional Josephson junction arrays, *Phys. Rev. B*, accepted, 1994.

[19] A. Barone and G. Paterno, *Physics and applications of the Josephson effect.* New York: John Wiley & Sons, chapter 11, 1982.